remote sensing

MDPI

Article

Salt Stockpile Inventory Management Using LiDAR Volumetric Measurements

Justin Anthony Mahlberg [1], Raja Manish [1], Yerassyl Koshan [1], Mina Joseph [1], Jidong Liu [1], Timothy Wells [2], Jeremy McGuffey [2], Ayman Habib [1] and Darcy M. Bullock [1,*]

[1] Joint Transportation Research Program, Purdue University, West Lafayette, IN 47907, USA
[2] Indiana Department of Transportation, 100 N Senate Ave, Marion County, Indianapolis, IN 46204, USA
* Correspondence: darcy@purdue.edu

Abstract: Transportation agencies in northern environments spend a considerable amount of their budget on salt for winter operations. For example, in the state of Indiana, there are approximately 140 salt storage facilities distributed throughout the state and the state expends between USD 30 M and USD 60 M on inventory and delivery each year. Historical techniques of relying on visual estimates of salt stockpiles can be inaccurate and do not scale well for managing the supply chain during the winter or planning for re-supply during summer months. This paper describes the implementation of a portable pole mounted LiDAR system that can be used to inventory a large barn in under 15 min and describes how this system has been deployed over 90 times at 30 facilities. A quick and easy accuracy test, based upon conservation of volume, was used to provide an independent check on the system performance by repositioning portions of the salt pile. Those tests indicated stockpile volumes can be estimated with an accuracy of approximately 0.1%. The paper concludes by discussing how this technology can be permanently installed near the roof for systematic monitoring throughout the year.

Keywords: winter operations; salt; management; stockpile; weather; LiDAR

Citation: Mahlberg, J.A.; Manish, R.; Koshan, Y.; Joseph, M.; Liu, J.; Wells, T.; McGuffey, J.; Habib, A.; Bullock, D.M. Salt Stockpile Inventory Management Using LiDAR Volumetric Measurements. *Remote Sens.* **2022**, *14*, 4802. https://doi.org/10.3390/rs14194802

Academic Editors: Lin Li, Mengjun Kang and Min Weng

Received: 8 August 2022
Accepted: 19 September 2022
Published: 26 September 2022

1. Introduction

Winter maintenance operations typically include the use of de-icing materials with a heavy reliance on road salt. Across the United States, over 70% of the population live in a region that experience winter weather conditions [1,2]. The use of road salt reduces and mitigates winter weather impacts and has increased over the decades with about 20 million tons of road salt used in the US per year [3–5]. Recent studies have shown that the use of de-icing salts have been impacting the biodiversity and fresh-water ecosystems due to a rise in salinity [1,6,7]. This environmental impact merged with the fiscal accountability and necessity to ensure proper mobility standards paves the way for future roadway de-icing measures [8–10].

Many agencies have moved away from traditional salt storage methods which were uncovered, outdoor facilities due to the loss of material and environmental impacts during precipitation events, some states even enforce the use of covered salt stockpiles [11–14]. Covered facilities for stockpiles make it difficult for evaluation of stockpiles through field surveys in an efficient manner due to limited access, poor lighting, and Global Navigation Satellite Signal (GNSS) accessibility is limited for Real-Time Kinematic (RTK) surveys [15–17]. The use of unmanned aerial vehicles (UAVs) has been crucial for stockpile estimation in open environments as they are a quick and safe method to acquire stockpile data [16,18–23]. The use of UAVs in indoor facilities are restricted due to minimal GNSS signal and obstacles in the flight path. All of the limitations in volume estimation of salt stockpiles cause inaccuracies and do not scale well for managing the supply chain during the winter or planning for re-supply during summer months.

2. Motivation

The Indiana Department of Transportation (INDOT) spends a considerable amount of their annual budget on salt for winter operations. Annually, anywhere from USD 30 million to USD 60 million of their operating budget is allocated for salt material and delivery, which is then distributed among their 140 facilities statewide. Figure 1 shows the strategic location of salt storage and maintenance facilities statewide, evenly spaced and generally located near interstate or US routes.

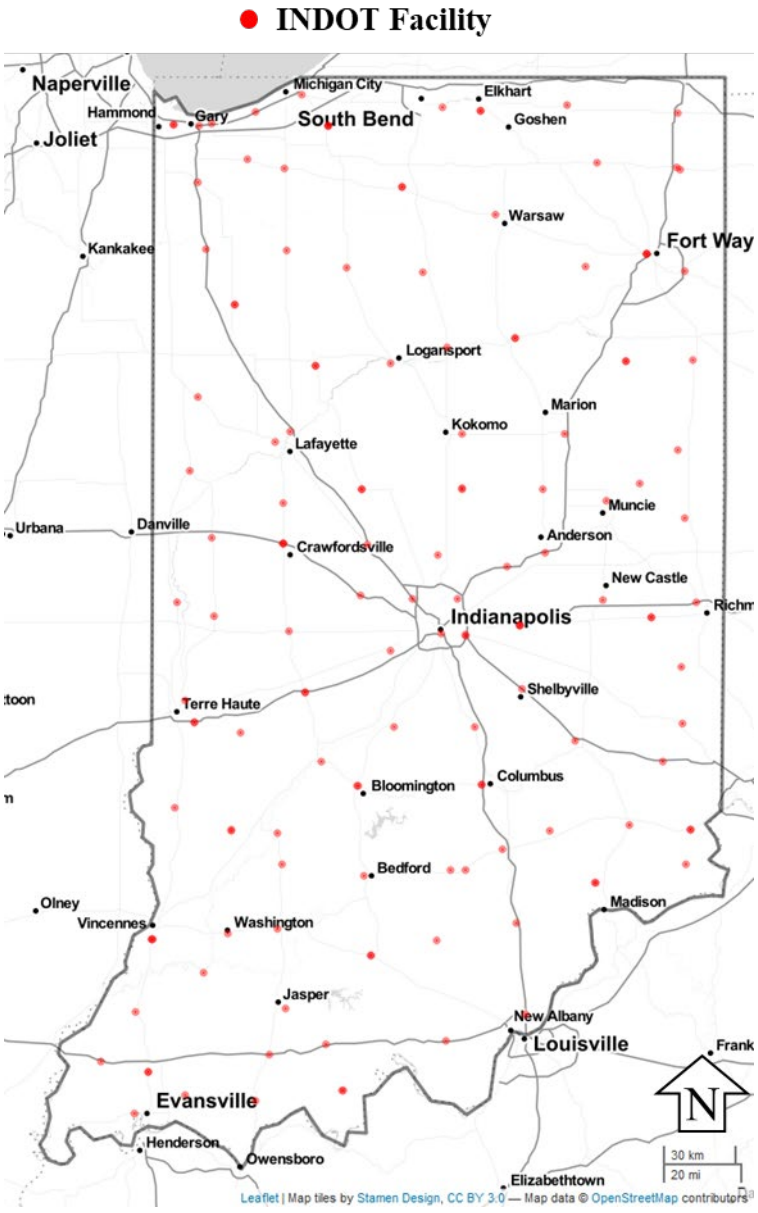

Figure 1. INDOT salt storage facilities and maintenance units.

One of the challenges the agency faces is each facility has different storage building sizes and types, which lead to unique storage capacities that preclude developing systematic visual inventory techniques, such as observing stockpile size to determine its volume. This estimation can also vary due to different visual perceptions and human errors [24,25]. An example of four different salt storage facilities can be observed in Figure 2 below. Figure 2a shows the facility in Sellersburg, Indiana which is a salt dome attached to a salt barn, Figure 2b is the Bloomington, Indiana facility consisting of a rectangular wooden structure with an open end on one side and a complementing salt dome adjacent to the

wooden structure. Figure 2c is the Gary, Indiana facility which is a rectangular concrete and steel barn structure and Figure 2d is a rectangular concrete and tension fabric structure in Rensselaer, Indiana. These unique structures are only representative of few configurations out of the 140 facilities INDOT has. The capacity and inventory in each facility becomes especially crucial during the winter season to prevent unnecessary delivery of material, prevent facilities from running out of salt mid-storm, and for reporting material application during the storm/season.

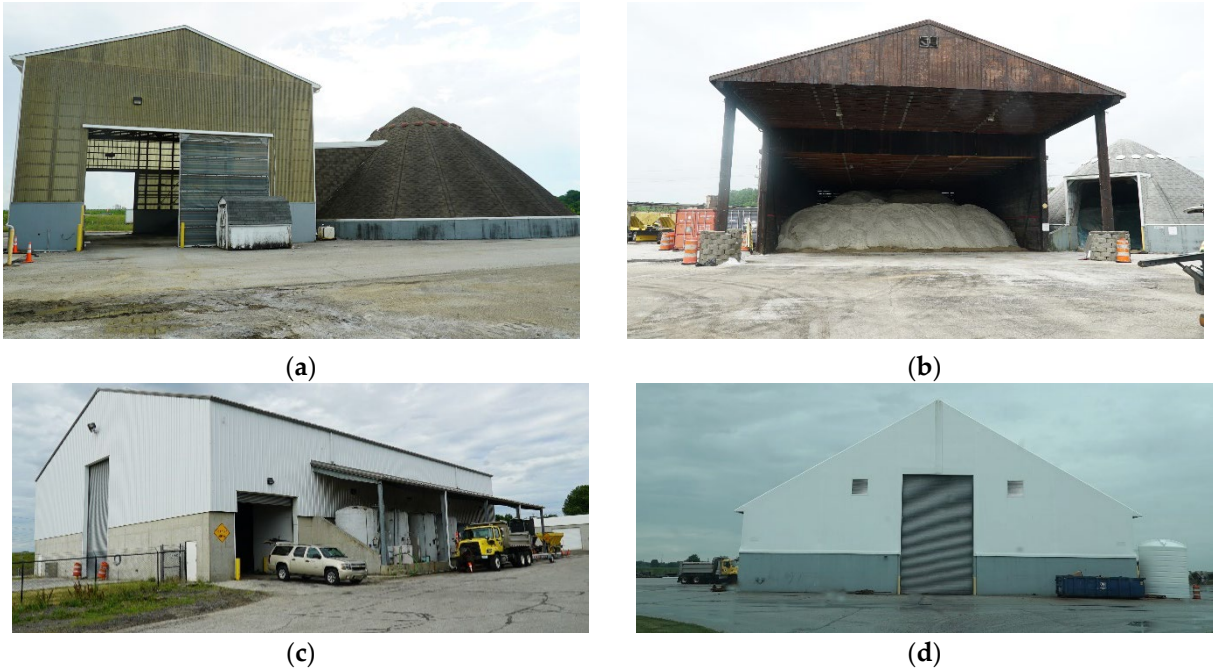

Figure 2. Examples of distinct INDOT salt storage facilities. (**a**) Sellersburg, Indiana Salt Facility (**b**) Bloomington, Indiana Salt Facility (**c**) Gary, Indiana Salt Facility (**d**) Rensselaer, Indiana Salt Facility.

Traditional methods for determining salt inventory include counting the amount of truck loads using/delivering salt, manual field surveys, and recent emerging technology: camera-based photogrammetry. Tracking material by truck load and even manual field surveys do not provide sufficient accuracy for season long inventory management data. Photogrammetric systems can be expensive and can also be problematic due to low-lighting conditions and occlusions or areas that are not visible to the camera.

3. Objectives

The objective of this study is to describe the deployment of a LiDAR based Stockpile Management and Reporting Technology (SMART) system, and to explain the data and visualization tools that were employed during a season long deployment. This study collected data at over 30 unique facilities and had a total of 88 scans to monitor salt usage over the winter season.

4. Smart System, Data Collection and Processing Methodology

4.1. SMART System

There are several key components for the SMART System to be operational and portable. The system, outfitted with all its components, can be seen in Figure 3 below. The compact design makes the system easy to transport and convenient to collect data anywhere. The primary components of the system, as observed in Figure 3a, are a GoPro Hero 9 RGB camera (callout *i*), and two Velodyne VLP-16 LiDAR sensors (callout *ii*). The two LiDAR sensors, with different coverage areas, provide a greater point density,

increased redundancy, and occlusion reduction compared to a single unit. Figure 3b shows the portable tripod that is used and the quick connect PVC/Polyvinyl chloride connection for fast and easy setup (callout *iii*). The remaining components can be observed in Figure 3c in the traveling case, which includes the power source (callout *iv*), and the user interface tablet (callout *v*).

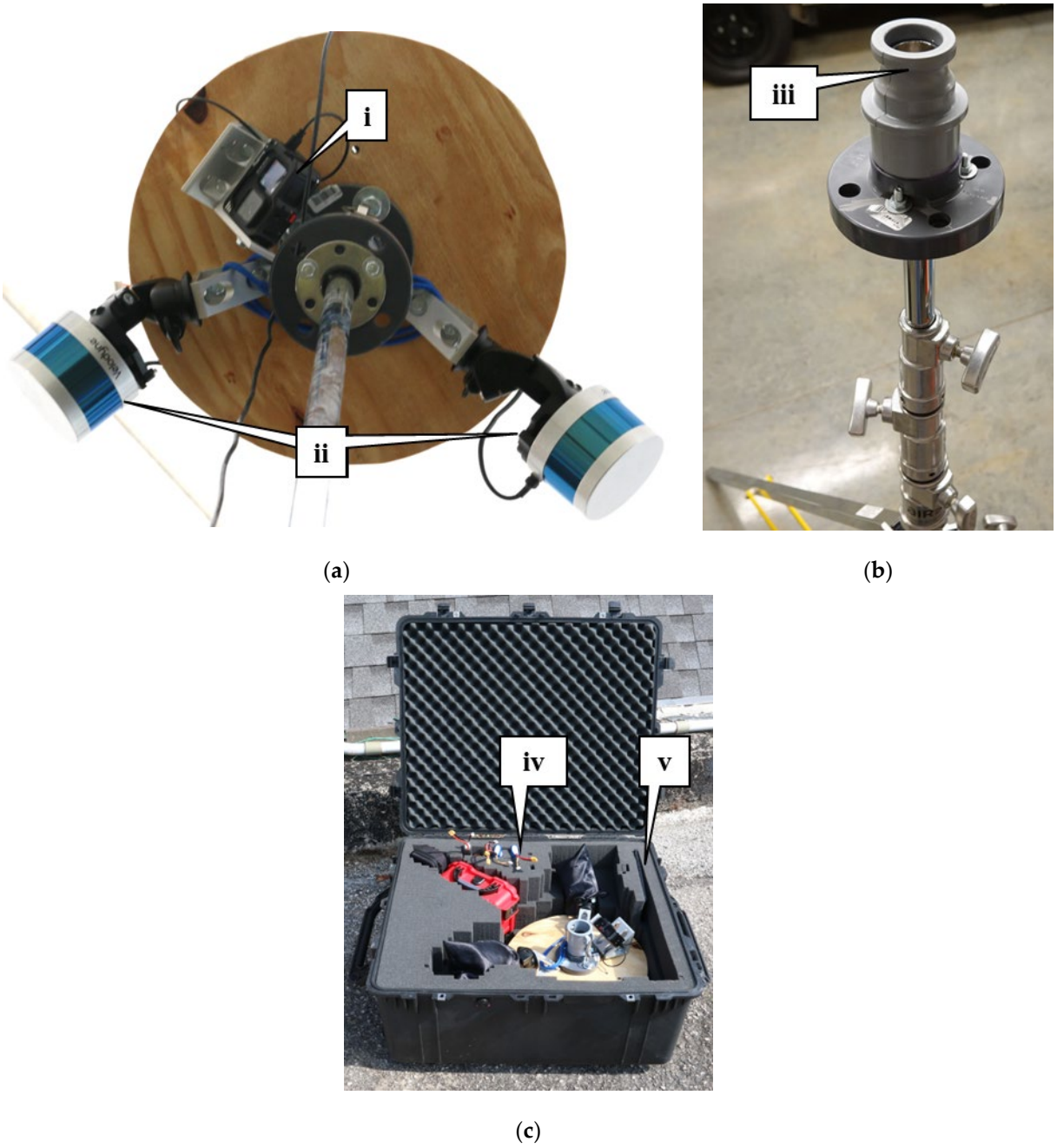

(**a**) (**b**)

(**c**)

Figure 3. The SMART system for data acquisition (**a**) SMART System (**b**) SMART Portable Tripod (**c**) SMART System Packaging for Portability.

4.2. SMART Data Collection and Processing Methodology

The SMART system's development, data acquisition procedure, and data processing strategy in this study are based on an early prototype system proposed by Manish et al., 2022 [26]. Figure 4 illustrates their proposed approach. When conducting an onsite data acquisition, the SMART system is placed on the tripod for scanning. Due to the limited field

of view of the camera and LiDAR sensors, the system is rotated manually at a clockwise increment of 30 degrees (as illustrated in Figure 4a) to capture data points enough to cover the stockpile. The orientation of the LiDAR units and camera require the 30-degree rotation to be performed 7 times with LiDAR capturing 10-s-long scans. This results in LiDAR/RGB data collected over 180 degrees of rotation, the first scan being at 0 degree and the final scan 180 degrees from the first. With two LiDAR units, the procedure collectively obtains a complete 360-degree scan of the facility. Depending on the size of the stockpile, not all areas of the pile may be visible to the system at a given location which would motivate the use of multiple stations for data collection.

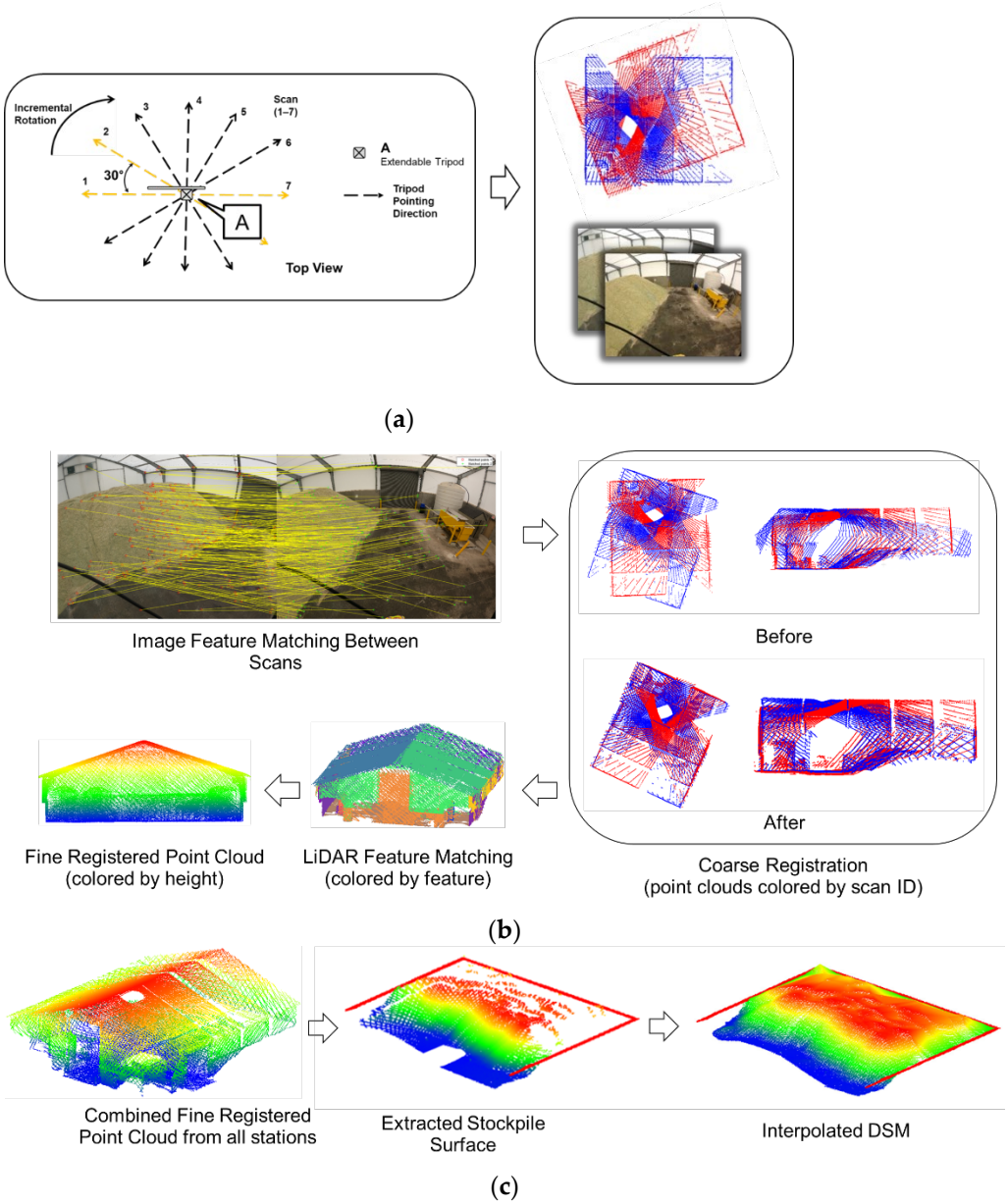

Figure 4. SMART data acquisition and processing methodology (**a**) diagram of system rotation for data collection (**b**) coarse registration of LiDAR scans (**c**) digital surface model of stockpile area.

After the data collection, the team uses the techniques from Manish et al., 2022 to perform coarse and fine registrations of point clouds which are then used to determine the stockpile volume [26]. As visualized in Figure 4b, at first, an image-assisted coarse registration of LiDAR scans is conducted wherein successive images are utilized to obtain scan-to-scan transformation through constrained iterative matching of Scale Invariant

Feature Transform (SIFT) features in two successive images at a time. The iterative matching avoids wrong matches due to the homogeneity of stockpile surface. Once the LiDAR scans are coarsely registered, all the individual scans are segmented to extract planar features, which are matched across the different scans. Then, a final optimization routine based on least squares adjustment is initiated for a feature-based fine registration of all scans [27]). If more than one station was collected at a facility, then the fine registered scans from each location are used to perform a coarse registration of all stations using a boundary tracing and identified minimum bounding rectangle methods for the registered scans at the individual stations [28,29]. The multi-station coarse registration is then followed by a fine registration using matched planar features in the combined multi-station scans. Finally, to compute the stockpile volume, the multi-station fine registered point clouds are levelled until the ground of the facility aligns with the XY plane. Then, a digital surface model (DSM) is generated by defining grid cells of identical size (0.1 m $\times$ 0.1 m in this research) uniformly in the XY plane right over the stockpile area within the boundary of the facility, as shown in Figure 4c. Each cell is assigned a height at the center of the cell based on a bilinear interpolated of the LiDAR surface of the stockpile (this interpolation establishes stockpile surface in occluded areas).

It is worth noting that when generating the DSM for a given facility, the number of grid cells will depend on the cell size, as mentioned above. The cell size will, in turn, affect data processing time–the smaller the cell, the more expensive it will be in terms of computation needed to generate the DSM. The selection of the cell size (0.1 m $\times$ 0.1 m) in this research did not result in a significant processing overhead. On a computer with an 8 core Intel i5 processor and 8 GB RAM, the DSM generation typically took about 30 s or less.

5. Study Locations

To capture a diverse portfolio of locations 26 INDOT facilities, and 4 local agency facilities were scanned. This diversity provided a magnitude of different challenges to ensure the system could accurately capture data in all facilities. Table 1 below summarizes the facilities that were scanned and the number of times the data collection team visited to capture data for a given facility. It can be noted that 88 total surveys were collected and 12 of those facilities were frequently traveled to, for observing changes in salt inventory over the winter season. Figure 5 shows, spatially, the scanning coverage across the state of Indiana. Each representative callout on the map is the respective facility from Table 1.

Table 1. Summary of data collections at each facility.

Map Ref.	Facility Name	# of Surveys	Map Ref.	Facility Name	# of Surveys
1	Crawfordsville	6	16	Rochester Unit	1
2	Lebanon	10	17	Greensburg Unit	1
3	Frankfort	6	18	Brookville Unit	1
4	Romney	6	19	Aurora Sub	1
5	West Lafayette River Road	4	20	Scottsburg Unit	1
6	Rensselaer	6	21	Sellersburg Unit-1	1
7	Chesterton	5	22	Sellersburg Unit-2	1
8	Michigan City	5	23	Corydon Unit	1
9	Miller	5	24	Salem Unit	1
10	Monticello	9	25	Bloomington Sub-1	1
11	US231	8	26	Bloomington Sub-2	1
12	City of Lafayette	3	27	Columbus Sub	1
13	City of West Lafayette Street Department	1	28	Portland Unit	1
14	LaPorte Unit	1	29	Valparaiso Unit	2
15	Plymouth Unit	1	30	Valparaiso Unit 2	3

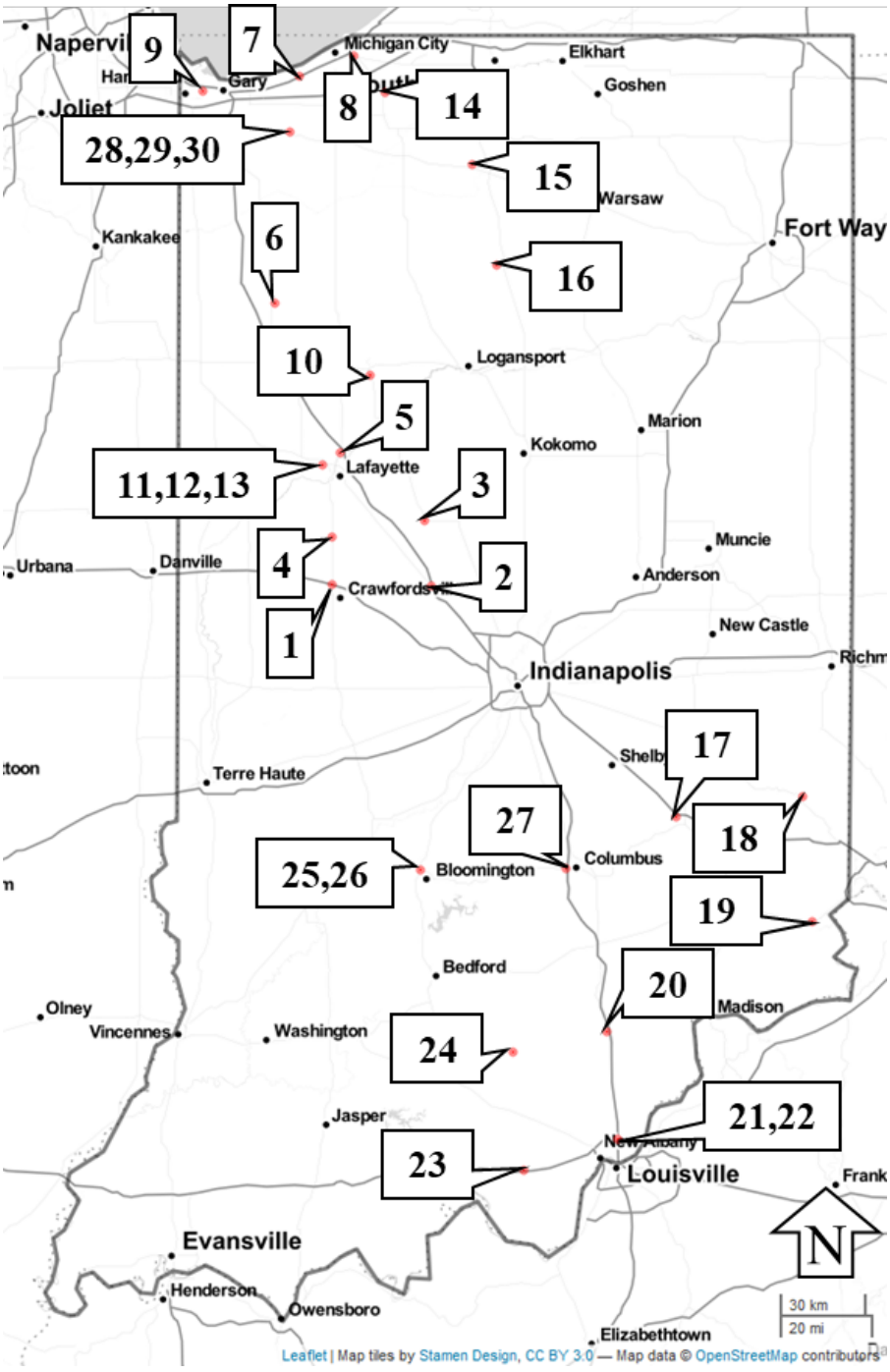

Figure 5. Locations of data collections across Indiana.

6. 2021–2022 Winter Monitoring and Results

To monitor the salt stockpile inventory fluctuation, the data collection team visited the same 12 facilities multiple times after salt deliveries and before/after a winter storm event. These facilities were chosen due to their frequency of experiencing winter storm events, and they include some of the largest salt storage facilities in the state. Table 2 below shows the 12 facilities that were monitored over the winter season and the amount of salt that was onsite at the time of the SMART salt scan.

Table 2. Salt pile inventory in cubic yards over the 2021–2022 winter season.

Name	Dates Collected																					
	Apr 30, 2021	Jun 08, 2021	Jun 23, 2021	Jul 22, 2021	Oct 12, 2021	Nov 23, 2021	Nov 24, 2021	Dec 07, 2021	Dec 17, 2021	Jan 04, 2022	Jan 06, 2022	Jan 19, 2022	Jan 26, 2022	Jan 28, 2022	Feb 09, 2022	Feb 11, 2022	Feb 14, 2022	Feb 16, 2022	Feb 23, 2022	Mar 31, 2022	May 23, 2022	Jun 13, 2022	Jun 14, 2022
Romney						715					1137		1099			417			519			1216	
Crawfordsville						2244					2246		1706			1354			931			2557	
Lebanon	1995				1882	1897					1788		1305			1053			2408	2156	3276	3255	
Frankfort						2509					2408		2179			1507			1290			3229	
Monticello								3004				3626						2862	2536			3571	
WL River Rd						1082						1899				857						1176	
WL 231	1266	1439		1307					1338			1294			1324	1322			1127			1022	
City of Lafayette		1789										1729						1495					
Rensselaer																910			1010				
Miller			3159				4438	4750		4335							3440						5295
Chesterton			2710					2620		2112							2596						3215
Michigan City			4259					4025		3639							3165						5488

Cubic Meters = (Cubic Yards)/1.308.

A representation for salt over the course of a winter season in Lebanon, Indiana can be seen in Figure 6. The first scan of the season was taken 23 November 2021 and had 1897 cubic yards (1450 cubic m) of salt in the facility. The next scan was taken on 6 January after the first snow event in the area which occurred on 2 January 2022, providing the first opportunity to scan after a winter event with a volume of 1788 cubic yards (1367 cubic meters). The team continued to monitor the salt after snow events on 26 January, 11 February, 23 February, 31 March, and at the end of the season on 23 May and 13 June 2022.

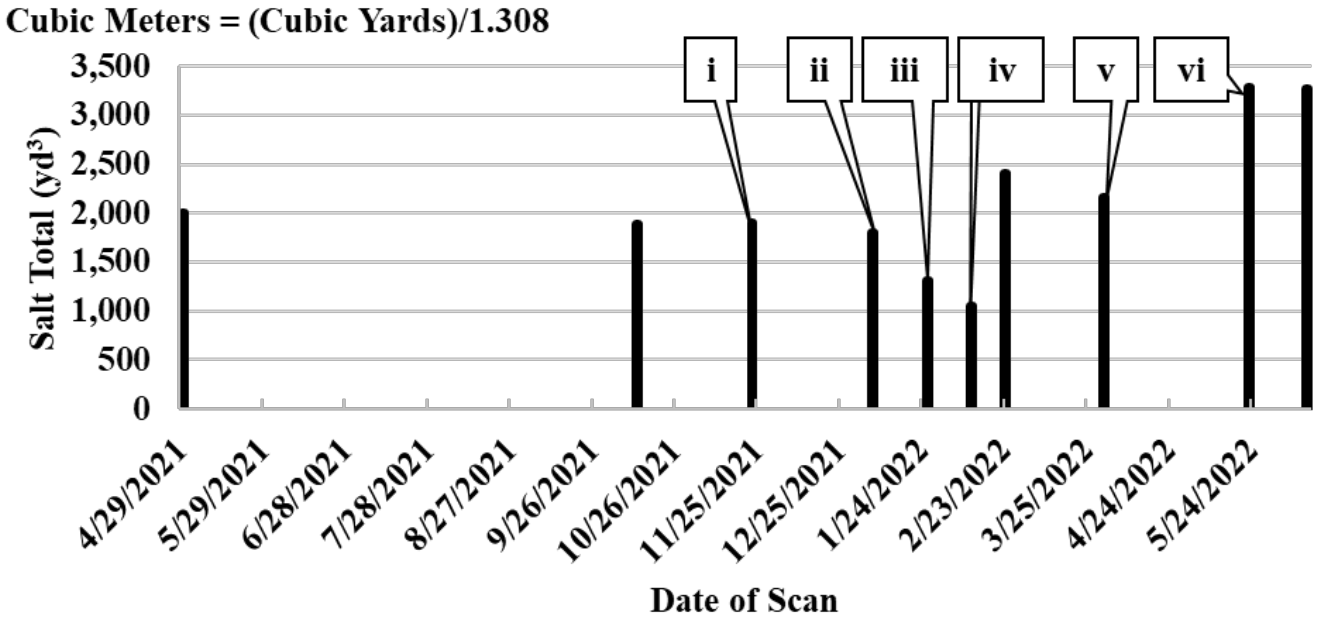

Figure 6. Total salt over the winter season in the Lebanon, Indiana salt facility.

Monitoring the amount of salt over the winter season reveals trends during winter storm events, and when the facility received a salt delivery. This information is important to agencies as it will enable them to actively monitor their salt usage before and after a winter event. This information can also be used for determining the quantity of additional salt that should be ordered. Callouts i–vi illustrated in Figure 6 can be seen as a DSM in Figure 7 below. These visuals are created in Cloud Compare from fine registered point clouds which are colorized by height [30]. Blue represents the ground surface and red represents the top of the salt pile which is approximately 4 m high. Figure 7a corresponds to callout i in Figure 6, Figure 7b to callout ii, Figure 7c to iii, Figure 7d to iv, Figure 7e to v, and Figure 7f to vi. The largest difference in salt totals can be observed between Figure 7d where the salt total is at, 053, Figure 7e where the total is 2408, and Figure 7f where the salt total is 3276.

Figure 8 shows the representative camera images of the salt stockpiles. These images show the removal and refill of material over time-from the untampered "white" appearing salt in the early days to the green salt in the middle, and the refilled stockpile at the end. It should be noted that the salt may have varying color depending on added chemicals or fading of the top layer over time. Figure 7a aligns with Figure 8a, along with the remaining Figures. Similar to Figure 7, the largest difference in salt totals can be observed between Figure 8d–f.

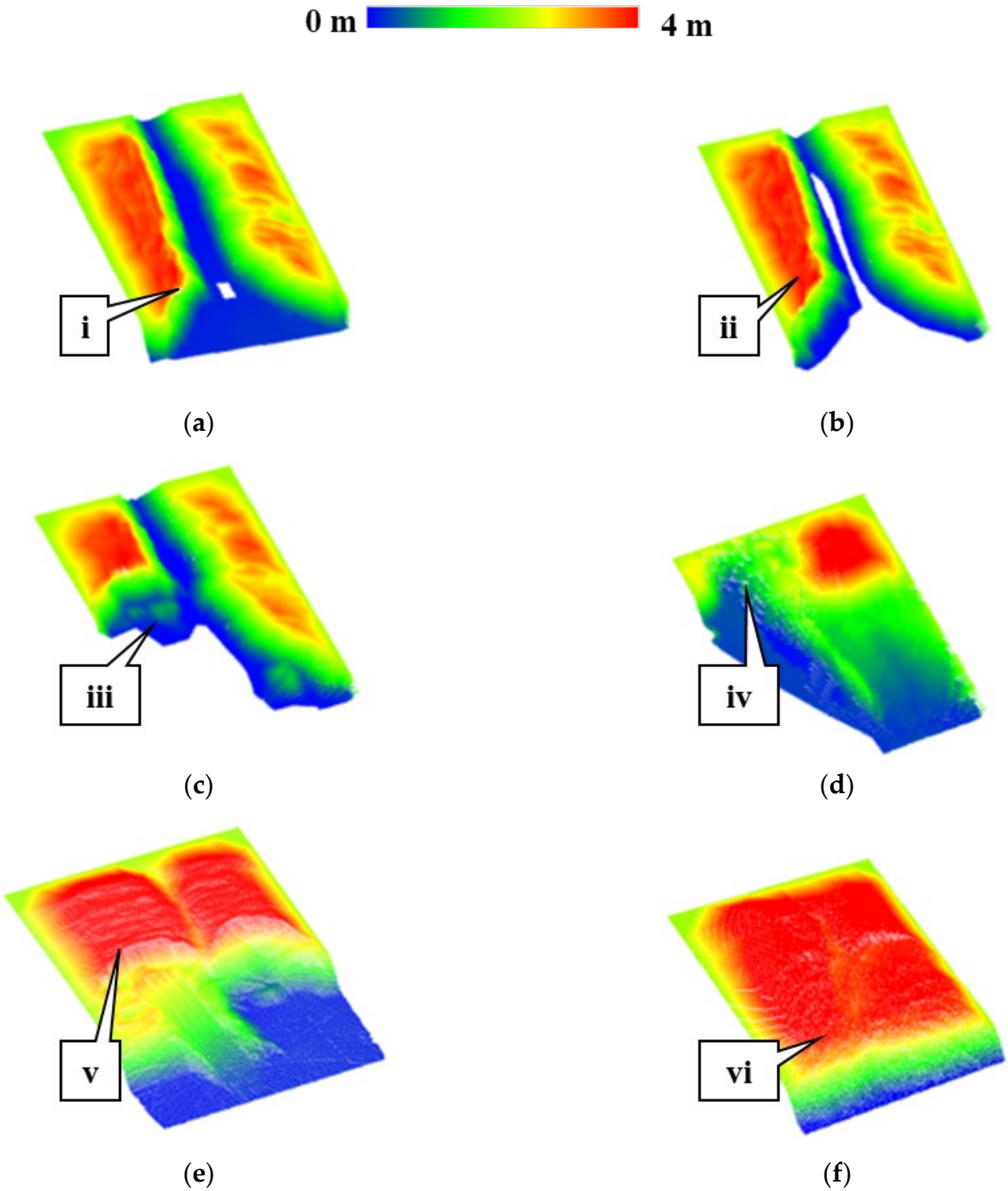

Figure 7. Digital surface models of Lebanon salt over 2021–2022 winter season (**a**) 23 November 2021, Digital Surface Model (**b**) 6 January 2022, Digital Surface Model (**c**) 26 January 2022, Digital Surface Model (**d**) 11 February 2022, Digital Surface Model (**e**) 31 March 2022, Digital Surface Model (**f**) 23 May 2022, Digital Surface Model.

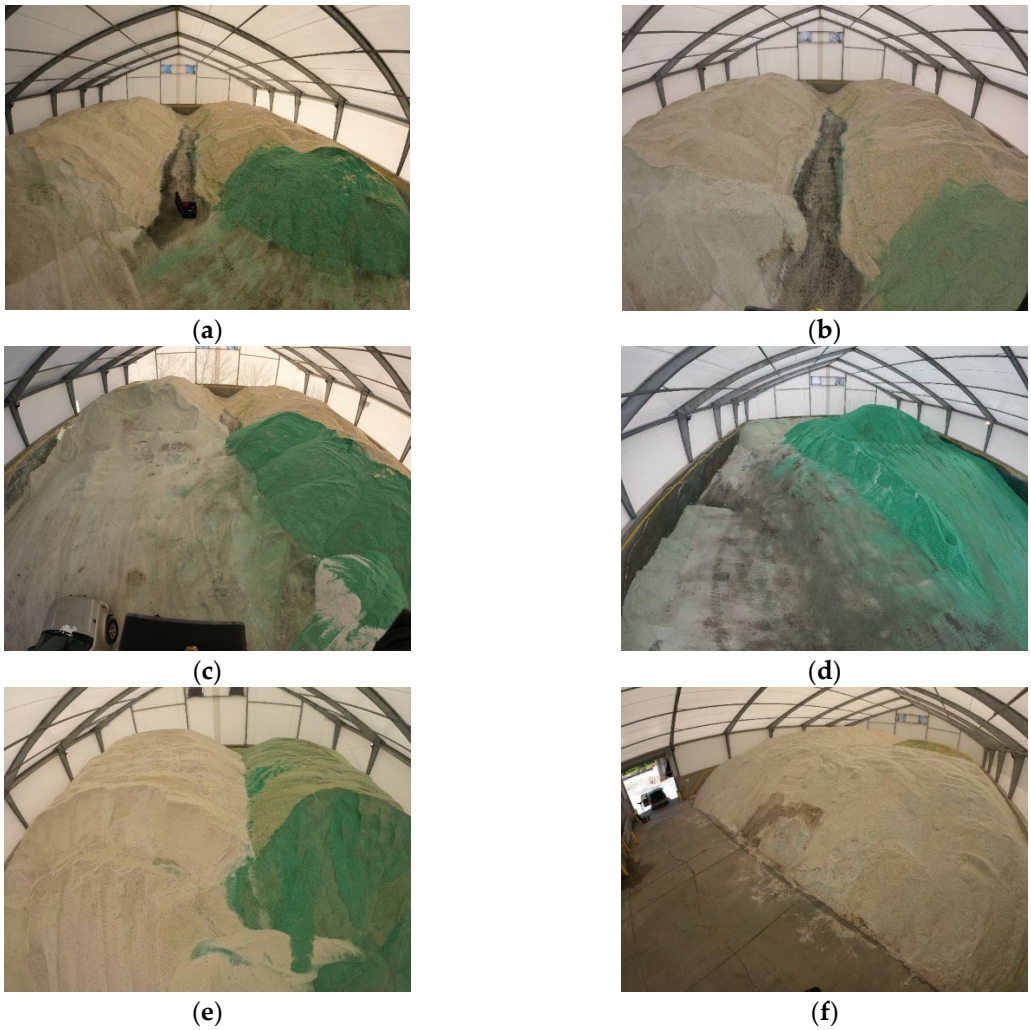

Figure 8. GoPro Images of corresponding Lebanon salt piles for the 2021–2022 winter season (**a**) 23 November 2021, GoPro Image (**b**) 6 January 2022, GoPro Image (**c**) 26 January 2022, GoPro Image (**d**) 11 February 2022, GoPro Image (**e**) 31 March 2022, GoPro Image (**f**) 23 May 2022, GoPro Image.

7. Field Deployment

The success and learning opportunities of the portable system over the 2021–2022 winter season has generated interest in a permanent SMART system installation in facilities. This would enable the agency to observe salt amounts in near real time from any location. Before mounting the system, a preliminary test was conducted to determine the optimal location for the SMART system. Figure 9a shows the temporary mounting of the unit on a mobile boom lift. Scans at three different mounting locations were performed to determine the optimal location. Figure 9b shows the three locations relative to the salt pile that were tested in the facility. The optimal location is shown as the red dot which provided the most coverage of the pile, while still capturing the front of the pile where most of the salt is removed. This position, at the time of the scan, was located towards the front of the pile but as the agency refills the barn, the system will be closer to the center of the pile. Additionally, this location provides visual to the LiDAR units and the camera of the back of the pile and an optimal view of the front of the pile where the amount of salt changes the most. The horizontal line in Figure 9b represents the center steel support in the salt barn and the three vertical lines represents the support truss to which the SMART system could be mounted. Additionally, the area in the front of the barn is an entryway used for storage, equipment, and loading, which is excluded from the salt pile estimation calculations.

(**a**)

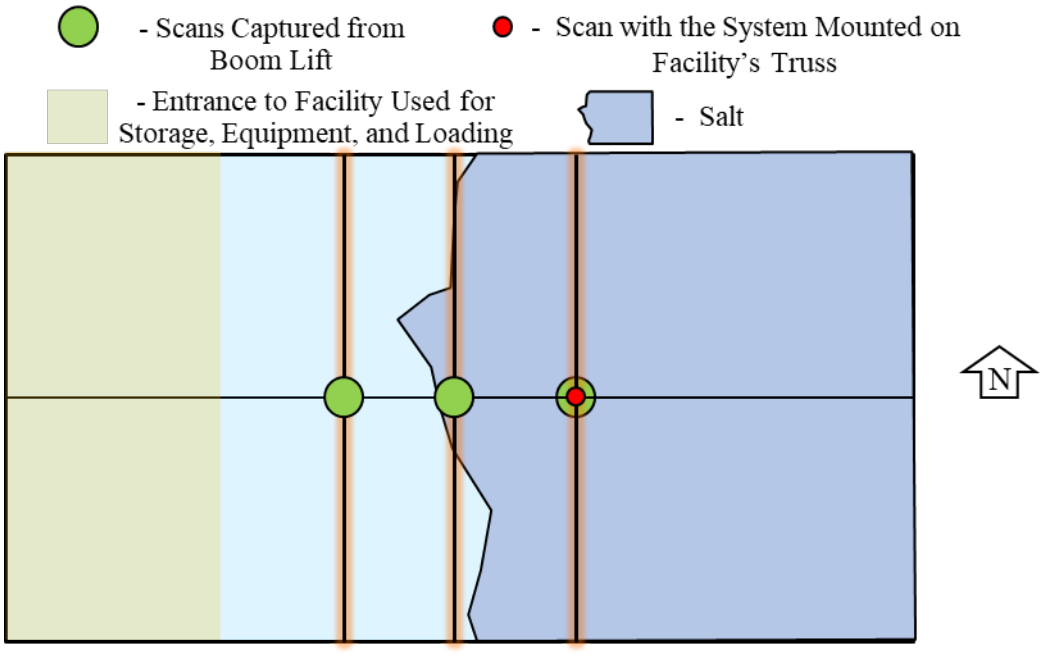

(**b**)

Figure 9. Testing locations for optimal permanent installation (**a**) Installation and Data Collection on Boom Lift (**b**) Location of Scans Relative to Salt Pile.

The system was mounted in the Lebanon salt barn (Figure 10a) and salt dome (Figure 10b). The functionality still worked the same as the portable unit except now there is a rotating motor, seen as callout i in Figure 10, to perform a 270-degree rotation for scanning at 30-degree increments, without overlap. This motor provided greater coverage of the storage facility, improved coarse registration quality, and reduced estimation errors, some of which were also observed in similar studies [31,32]. Mounting the system at the peak of the structure increased visibility by 10% making only 25% of the whole pile not visible to the system which provides more accurate estimates. The percent not visible to the system can be minimized by pruning the peaks of salt while piling. Nonetheless, the volume estimation procedure is not a serious concern since the interpolation is still able

to calculate an accurate estimate of the stockpile. The accuracy was also verified through terrestrial laser scanning [26].

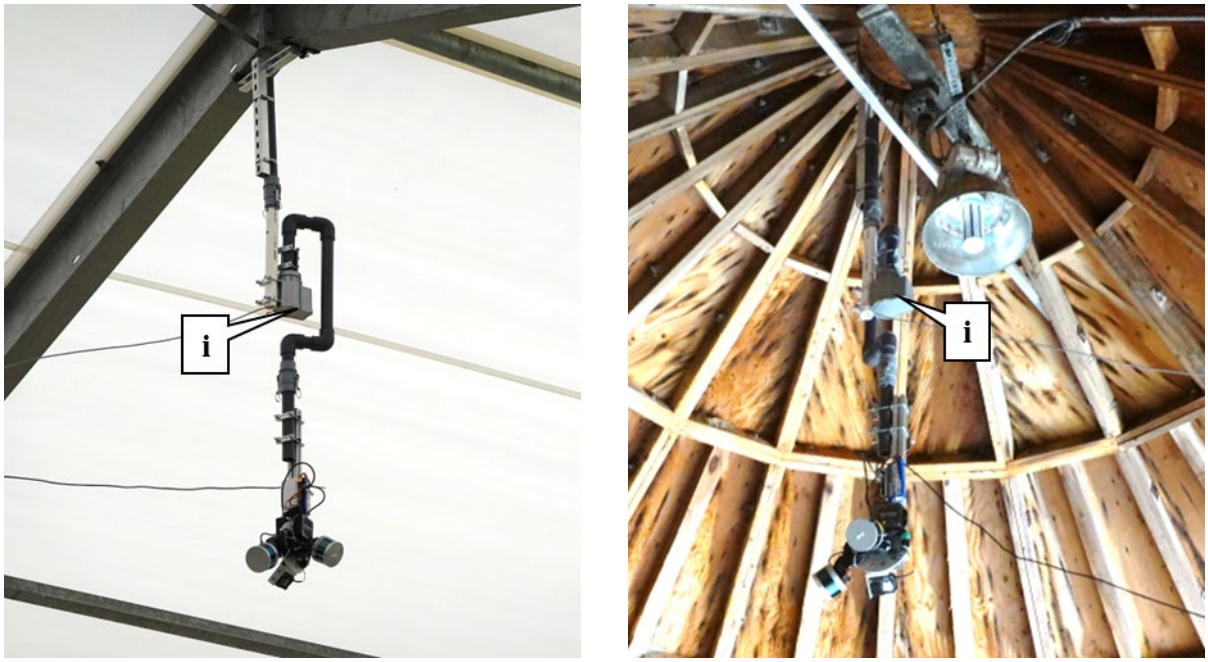

(**a**) (**b**)

Figure 10. Permanent installation of the SMART system (**a**) Permanent Installation in a Salt Barn (**b**) Permanent Installation in a Salt Dome.

8. Field Validation of Volume

The principles of conservation of volume are used to provide a quick test of the system. To determine and validate the accuracy of the SMART salt system, a salt repositioning test was performed. This test collected data in a series of four scans with the permanent installation in the salt barn. The initial scan can be seen in a GoPro image collected directly from the system as Figure 11a and as a digital surface model from the processed point clouds in Cloud Compare as Figure 11b [30]. This serves as the baseline volume for the following three scans. The total volume is 2156 cubic yards (1648 cubic meters). A payloader moved five buckets of salt from the initial stockpile to the front of the pile/facility (in the storage/loading area) to simulate the removal of salt for use on roadways, which can be seen as callout i in Figure 11c,d below. After scanning, the initial stockpile has 2149 cubic yards (1643 cubic meters) and the moved salt is 9 cubic yards (6 cubic meters) bringing the total to 2158 cubic yards (1649 cubic meters). From the original scan, this is a 0.09% error. Five additional buckets were removed from the initial pile making a total of 10 removed buckets. The moved salt is referenced as callout ii in the GoPro image (Figure 11e) and in the digital surface model (Figure 11f). The initial stockpile now has a volume of 2136 cubic yards (1633 cubic meters), and the moved salt has a volume of 21 cubic yards (16 cubic meters) making a total of 2157 cubic yards (1649 cubic meters) and a 0.04% error. The moved salt was then returned to the initial stockpile and rescanned seen in Figure 11g,h. The total volume is 2156 cubic yards (1648 cubic meters) which was identical to the initial scan, meaning a 0.00% error. This validation test proved effective in determining the accuracy of the SMART salt system as there was no error observed greater than 0.1%, vastly improving traditional methods of determining salt stockpile inventories, which inherently introduce a human interpretation/observation ambiguity/error.

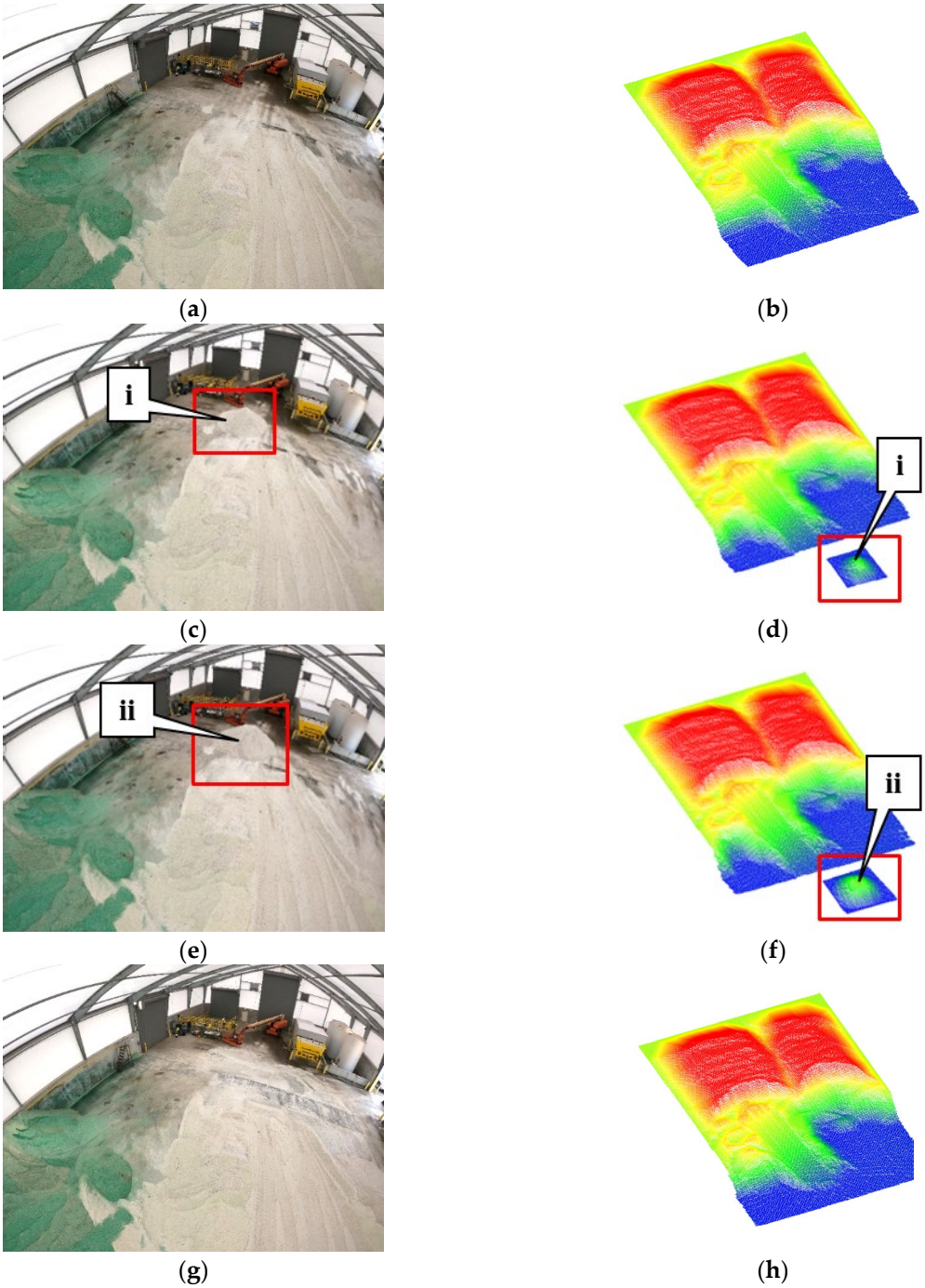

Figure 11. Data validation through salt repositioning (**a**) GoPro Image Before Salt Repositioning (**b**) Digital Surface Model Before Salt Repositioning (**c**) GoPro Image with 5 Buckets Repositioned (**d**) Digital Surface Model with 5 Buckets Repositioned (**e**) GoPro Image with 10 Buckets Repositioned (**f**) Digital Surface Model with 10 Buckets Repositioned (**g**) GoPro Image After Salt Repositioning (**h**) Digital Surface Model After Salt Repositioning.

9. Conclusions

This study showed the use and validation of the new Stockpile Monitoring and Reporting Technology (SMART) system that utilizes two LiDAR Sensors and a camera to determine accurate volume estimations of salt stockpiles. Using this system enables integrated visualizations of digital surface models and camera images to provide context to the accurate volume estimation. This portable or permanent system solves a large

logistical problem of salt stockpile management for the 140 INDOT facilities across the state. The portable system was utilized during the 2021–2022 winter season for regular monitoring of 12 facilities and almost 100 scans. The volume estimate error is less than 0.1%, providing the agency with a more concise and efficient method for determining stockpile quantities statewide.

The data this system delivers has the capability to provide the agency with a better understanding of salt usage during various parts of a winter storm and at all their facilities. The portable system provides versatility in not having a fixed asset in a barn. This system could be used to cover multiple facilities over the course of the winter and even be expanded for other stockpiles (e.g., asphalt, gravel, etc.) Another option with this system is a permanent installation, which would enable the agency to determine salt usage throughout a storm event and unit level usage. Additionally, this system could be integrated with the INDOT Management Information System (MIS) to provide notifications when stockpiles need replenishment or are at capacity to aid with stockpile delivery logistics. The system cost based on the current market rate of its components is about USD 10,000, and through various developmental phases, the data processing time to estimate volume has reduced from almost half day to under an hour. These costs currently only include the cost of the equipment. The computing time and process is still being improved, resulting in the annual cost of managing equipment and data to be reduced as well. Hence, with the increasing demand and reduction in the cost of LiDAR sensors, as well as further developments in hardware/software automation, the system is expected to become more cost-efficient and capable to provide end-users a near real-time volumetric assessment.

Author Contributions: Study conception and design: A.H., D.M.B., T.W. and J.M.; data collection: J.A.M., R.M., Y.K., M.J. and J.L.; analysis and interpretation of results: J.A.M., R.M., Y.K., M.J., J.L., A.H. and D.M.B.; draft manuscript preparation: J.A.M., Y.K., M.J., A.H. and D.M.B. All authors have read and agreed to the published version of the manuscript.

Funding: This work was supported by the Joint Transportation Research Program and the Indiana Department of Transportation.

Acknowledgments: The contents of this paper reflect the views of the authors, who are responsible for the facts and accuracy of the data presented herein, and do not necessarily reflect the official views or policies of the sponsoring organizations or data vendors. These contents do not constitute a standard, specification, or regulation.

Conflicts of Interest: The authors declare no conflict of interest.

References

1. Hintz, W.D.; Fay, L.; Relyea, R.A. Road Salts, Human Safety, and the Rising Salinity of Our Fresh Waters. *Front. Ecol. Environ.* **2022**, *20*, 22–30. [CrossRef]
2. Snow & Ice—FHWA Road Weather Management. Available online: https://ops.fhwa.dot.gov/weather/weather_events/snow_ice.htm (accessed on 7 July 2022).
3. Bagenstose, K. Winter Weather: Road Salt Use Degrading Roads, Bridges, Scientists Say. *USA Today* 2019. Available online: https://www.usatoday.com/story/news/nation/2019/12/24/winter-weather-road-salt-use-problems/2741286001/ (accessed on 14 June 2022).
4. Breining, G. We're Pouring Millions of Tons of Salt on Roads Each Winter. Here's Why That's a Problem. Ensia. Available online: https://ensia.com/features/road-salt/ (accessed on 7 July 2022).
5. Transportation Research Board. Highway Deicing Comparing Salt and Calcium Magnesium Acetate. *Highw. Deicing Spec. Rep.* **1991**, *235*, 16–30.
6. Kaushal, S.S.; Groffman, P.M.; Likens, G.E.; Belt, K.T.; Stack, W.P.; Kelly, V.R.; Band, L.E.; Fisher, G.T. Increased Salinization of Fresh Water in the Northeastern United States. *Proc. Natl. Acad. Sci. USA* **2005**, *102*, 13517–13520. [CrossRef] [PubMed]
7. Kelly, V.R.; Cunningham, M.A.; Curri, N.; Findlay, S.E.; Carroll, S.M. The Distribution of Road Salt in Private Drinking Water Wells in a Southeastern New York Suburban Township. *J. Environ. Quali.* **2018**, *47*, 445–451. [CrossRef] [PubMed]
8. Knapp, K.K.; Kroeger, D.; Giese, K. *Mobility and Safety Impacts of Winter Storm Events in a Freeway Environment*; Iowa State University: Ames, IA, USA, 2000.
9. Desai, J.; Mahlberg, J.; Kim, W.; Sakhare, R.; Li, H.; McGuffey, J.; Bullock, D.M. Leveraging Telematics for Winter Operations Performance Measures and Tactical Adjustment. *J. Transp. Technol.* **2021**, *11*, 611–627. [CrossRef]

10. Mahlberg, J.; Zhang, Y.; Jha, S.; Mathew, J.K.; Li, H.; Desai, J.; Kim, W.; McGuffey, J.; Wells, T.; Krogmeier, J.V.; et al. *Development of an Intelligent Snowplow Truck That Integrates Telematics Technology, Roadway Sensors, and Connected Vehicle*; Joint Transportation Research Program Publication No. FHWA/IN/JTRP-2021/27; Purdue University: West Lafayette, IN, USA, 2021. [CrossRef]
11. Kasich, J.R.; Tayler, M. *Recommendations for Salt Storage*; Ohio's Water Resources Council: Columbus, OH, USA, 2013; p. 25.
12. Ohno, T. Levels of Total Cyanide and NaCl in Surface Waters Adjacent to Road Salt Storage Facilities. *Environ. Pollut.* **1990**, *67*, 123–132. [CrossRef]
13. Safe and Sustainable Salt Storage. Salt Storage Handbook. Available online: http://www.nwpa.us/uploads/1/2/9/8/129889926/salt-institute-salt-storage-handbook.pdf (accessed on 5 April 2022).
14. Mass.Gov. Guidelines on Road Salt Storage. Massachusetts Department of Environmental Protection. Available online: https://www.mass.gov/guides/guidelines-on-road-salt-storage (accessed on 7 July 2022).
15. Yilmaz, H.M. Close Range Photogrammetry in Volume Computing. *Exp. Tech.* **2010**, *34*, 48–54. [CrossRef]
16. He, H.; Chen, T.; Zeng, H.; Huang, S. Ground Control Point-Free Unmanned Aerial Vehicle-Based Photogrammetry for Volume Estimation of Stockpiles Carried on Barges. *Sensors* **2019**, *19*, 3534. [CrossRef] [PubMed]
17. SenseFly. Speed, Efficiency & Accuracy in Stockpile Surveying. Available online: https://www.sensefly.com/blog/achieving-greater-speed-efficiency-amp-accuracy-in-stockpile-surveying-with-ebee-x/ (accessed on 25 August 2022).
18. Mora, O.E.; Chen, J.; Stoiber, P.; Koppanyi, Z.; Pluta, D.; Josenhans, R.; Okubo, M. Accuracy of Stockpile Estimates Using Low-Cost sUAS Photogrammetry. *Int. J. Remote Sens.* **2020**, *41*, 4512–4529. [CrossRef]
19. Hugenholtz, C.H.; Walker, J.; Brown, O.; Myshak, S. Earthwork Volumetrics with an Unmanned Aerial Vehicle and Softcopy Photogrammetry. *J. Surv. Eng.* **2015**, *141*, 06014003. [CrossRef]
20. Ajayi, O.G.; Ajulo, J. Investigating the Applicability of Unmanned Aerial Vehicles (UAV) Photogrammetry for the Estimation of the Volume of Stockpiles. *Quaest. Geogr.* **2021**, *40*, 25–38. [CrossRef]
21. Zhu, J.; Yang, J.; Fan, J.; Danni, A.; Jiang, Y.; Song, H.; Wang, Y. Accurate Measurement of Granary Stockpile Volume Based on Fast Registration of Multi-Station Scans. *Remote Sens. Lett.* **2018**, *9*, 569–577. [CrossRef]
22. Liu, S.; Yu, J.; Ke, Z.; Dai, F.; Chen, Y. Aerial–Ground Collaborative 3D Reconstruction for Fast Pile Volume Estimation with Unexplored Surroundings. *Int. J. Adv. Robot. Syst.* **2020**, *17*, 1729881420919948. [CrossRef]
23. Alsayed, A.; Yunusa-Kaltungo, A.; Quinn, M.K.; Arvin, F.; Nabawy, M.R.A. Drone-Assisted Confined Space Inspection and Stockpile Volume Estimation. *Remote Sens.* **2021**, *13*, 3356. [CrossRef]
24. Oliveira, A.; Oliveira, J.F.; Pereira, J.M.; de Araúo, B.R.; Boavida, J. 3D Modelling of Laser Scanned and Photogrammetric Data for Digital Documentation: The Mosteiro da Batalha Case Study. *J. Real-Time Image Proc.* **2014**, *9*, 673–688. [CrossRef]
25. Chekole, S.D. Surveying with GPS, Total Station, and Terrestrial Scanner: A Comparative Study. Master's Thesis, Royal Institute of Technology, Stockholm, Sweden, 2014. Available online: https://www.diva-portal.org/smash/get/diva2:715829/fulltext01.pdf (accessed on 16 March 2022).
26. Manish, R.; Hasheminasab, S.M.; Liu, J.; Koshan, Y.; Mahlberg, J.A.; Lin, Y.C.; Ravi, R.; Zhou, T.; McGuffey, J.; Wells, T.; et al. Image-Aided LiDAR Mapping Platform and Data Processing Strategy for Stockpile Volume Estimation. *Remote Sens.* **2022**, *14*, 231. [CrossRef]
27. Lin, Y.-C.; Liu, J.; Cheng, Y.-T.; Hasheminasab, S.M.; Wells, T.; Bullock, D.; Habib, A. Processing Strategy and Comparative Performance of Different Mobile LiDAR System Grades for Bridge Monitoring: A Case Study. *Sensors* **2021**, *21*, 7550. [CrossRef] [PubMed]
28. Sampath, A.; Shan, J. Building Boundary Tracing and Regularization from Airborne LiDAR Point Clouds. *Photogramm. Eng. Remote Sens.* **2007**, *73*, 805–812. [CrossRef]
29. Kwak, E.; Habib, A. Automatic Representation and Reconstruction of DBM from LiDAR Data Using Recursive Minimum Bounding Rectangle. *ISPRS J. Photogramm. Remote Sens.* **2014**, *93*, 171–191. [CrossRef]
30. CloudCompare, Version 2.6.1. GPL Software. 2022. Available online: http://www.cloudcompare.org/ (accessed on 22 March 2022).
31. Alsayed, A.; Nabawy, M.R.; Yunusa-Kaltungo, A.; Arvin, F.; Quinn, M.K. Enhancing 1D LiDAR Scanning for Accurate Stockpile Volume Estimation Within Drone-Based Mapping Systems. In Proceedings of the AIAA Aviation 2021 Forum, Virtual, 2–6 August 2021. [CrossRef]
32. 3D Stockpile Inventory—Pole Mounted or Inside Warehouse—EIP Enviro Controls. Available online: https://eipenviroindia.com/3d-stockpile-inventory-pole-mounted-or-inside-warehouse/ (accessed on 25 August 2022).